EC research
Industrial & Engineering Chemistry Research
pubs.acs.org/IECR
Article

First Measurements for the Simultaneous Sorption of Difluoromethane and Pentafluoroethane Mixtures in Ionic liquids Using the Integral Mass Balance Method

Kalin R. Baca, Darren P. Broom, Mark G. Roper, Michael J. Benham, and Mark B. Shiflett*

Cite This: *Ind. Eng. Chem. Res.* 2022, 61, 9774−9784
Read Online

ABSTRACT: Multicomponent absorption measurements are notoriously difficult both experimentally and analytically, which is why the literature is lacking information, even though the results are important for understanding real separation systems. In the case of designing a separation process for hydrofluorocarbon (HFC) refrigerant mixtures using an ionic liquid (IL), it is important to understand multicomponent effects; however, almost all published results are for single component HFC/IL systems. To address this challenge, new gravimetric microbalances utilizing the Integral Mass Balance (IMB) method have been designed by Hiden Isochema to efficiently and accurately measure multicomponent gas sorption in liquids with low volatility (e.g., ILs) and solids. The present work investigates the mixture absorption of difluoromethane (HFC-32) and pentafluoroethane (HFC-125) in two ILs (1-*n*-butyl-3-methylimidazolium tetrafluoroborate and 1-*n*-butyl-3-methylimidazolium hexafluorophosphate) at 298.15 K for the purpose of understanding HFC mixture/IL interactions. For the first time, these state-of-the-art instruments have allowed for the measurement of an HFC binary gas mixture in ILs that can be compared with existing single gas solubility measurements.

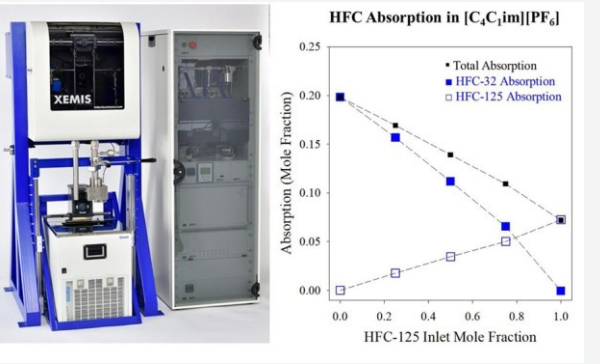

1. INTRODUCTION

Exciting, ground-breaking, and transformative research in science and engineering relies on access to state-of-the-art instrumentation and software. Gravimetric measurements of sorption behavior are critical for understanding physical and chemical properties to discover and develop new materials. The vast majority of sorption studies in the literature rely on single component, isothermal measurements using either gravimetric or volumetric techniques.[1] What is now required is multicomponent (competitive) sorption measurements under realistic operating conditions.

The main difficulty with multicomponent sorption measurements is the determination of the concentration of each species in the sorbed phase.[2] Total uptakes from mixtures may be measured gravimetrically, but the composition of the sorbed phase can only be determined indirectly by measuring the amount of each species removed from the gas phase.[3] This approach is limited by the sample size and the amount of sorption exhibited by the material. Similarly, volumetric techniques rely on the determination of the composition of a mixture in equilibrium with the solid, rather than the direct determination of the amount of each adsorbed component.[4]

Multicomponent measurements can also be very laborious.[5] Two traditional methods of measuring multicomponent adsorption involve using either open or closed volumetric systems.[6] Closed system measurements tend to be the most accurate, but are particularly time-consuming. The time required can be appreciated by considering that one measurement yields a single data point in terms of pressure, temperature, and composition (of either the bulk or sorbed phases), yet equilibrium may take several hours or days depending on the species, the adsorbent/catalyst, and the measurement conditions.[1,6]

These points constitute serious practical challenges to the efficient and accurate measurement of multicomponent gas sorption and have undoubtedly contributed to the shortage of comprehensive multicomponent sorption and kinetic data in the literature.[7] The number of materials being developed for sorption and catalysis applications and the laborious nature of multicomponent measurements means that the amount of data available is likely to remain small compared with the number of possible adsorbate−adsorbent combinations.[1] Models for the prediction of sorption for binary and higher mixtures from

Received: February 12, 2022
Revised: May 31, 2022
Accepted: June 5, 2022
Published: June 21, 2022

https://doi.org/10.1021/acs.iecr.2c00497
Ind. Eng. Chem. Res. 2022, 61, 9774−9784

single component data, such as the ideal adsorbed solution theory (IAST)[8,9] provide some information, but these models still require experimental multicomponent measurements for validation.[1]

The National Institute of Standards and Technology (NIST) published a report, Measurement Needs in the Adsorption Sciences in April 2015.[10] The report outlines the critical need to develop instrumentation and methods for characterizing materials using (1) *mixed gas systems*, (2) *dynamic conditions*, (3) *multitechnique approaches*, and (4) *small quantities* that combine sorption measurements with other analytical tools; therefore, complementary measurement techniques that can work together are needed such as ad(ab)sorption/desorption with mass spectroscopy. Kinetic and diffusion measurement techniques are also essential to evaluate (5) *nonequilibrium behavior of materials* and (6) *automated instrumentation* will increase the pace for optimization of variable sets.[10]

In light of this, a new technique for measuring multicomponent sorption, known as the Integral Mass Balance (IMB) method, was introduced recently by Broom et al.[11] It was demonstrated using a Hiden Isochema Intelligent Gravimetric Analyzer (IGA), but it has now also been implemented using a Hiden Isochema XEMIS microbalance as shown in Figure 1, which can operate over a wider pressure range than the IGA, and with corrosive species. The IGA + IMB and XEMIS + IMB methods are used here for the first time to measure binary sorption of HFCs in ILs.

Measuring binary and multicomponent sorption of HFCs in ILs is important in assessing the potential of ILs for separating refrigerant mixtures. The Montreal Protocol phased out chlorofluorocarbon (CFC) refrigerants because of their high ozone depletion potential (ODP).[12,13] The replacements, typically mixtures of hydrofluorocarbons (HFCs), are safe for the Earth's ozone layer, but some have been found to have high global warming potentials (GWPs).[12,13] As a result, 197 countries signed the Kigali agreement in 2016 to phase out the use of high GWP HFCs.[13] There are millions of tons of refrigerant mixtures that contain low-GWP compounds, but there are no good methods for separating and reclaiming the individual components, given that many mixtures are azeotropic or near-azeotropic. The market potential for recycling low-GWP refrigerants is valued at more than a billion U.S. dollars. In addition, preventing the incineration or release of high-GWP refrigerants in the U.S. would be equivalent to eliminating 175 million metric tons of CO_2 (or emissions from 50 million cars) annually. It is urgent to develop effective ways of separating, recycling, and repurposing HFCs, and the current $900 billion stimulus bill passed by Congress and signed by the President in December 2020 now requires the U.S. Environmental Protection Agency (EPA) to begin the phase out of HFCs under the American Innovation and Manufacturing Act (AIM Act).[14,15]

The measurements reported here will lay the groundwork for the design and development of an extractive distillation process using IL entrainers. Several papers have been published on single refrigerant gas sorption in ILs, but until now no mixture data has been available.[16−36] In this study, the simultaneous sorption, as a function of composition, of HFC-32 (CH_2F_2, difluoromethane) and HFC-125 (CHF_2CF_3, pentafluoroethane) in ILs 1-*n*-butyl-3-methylimidazolium tetrafluoroborate ($[C_4C_1im][BF_4]$) and 1-*n*-butyl-3-methylimidazolium hexafluorophosphate ($[C_4C_1im][PF_6]$) has been measured for the first time. We begin by providing a brief overview of conventional techniques for measuring multicomponent sorption equilibria for the characterization of sorbents for gas separations, before introducing the IMB method.

Figure 1. Hiden XEMIS gravimetric microbalance with IMB reactor.

2. CHARACTERIZING SORBENTS FOR SEPARATIONS

Separating gases using porous materials or absorbents usually relies on the selective sorption of one species over another.[8,9] Industrial separations require multicomponent gas sorption isotherms for complex process designs,[37] but obtaining such data is experimentally challenging.[2,6,38−41] The techniques used for measuring both adsorption by porous materials and absorption by liquid absorbents, such as ILs, for separations are broadly similar.

2.1. Traditional Techniques. Single component (pure gas) data are usually measured using gravimetric[42−45] or volumetric/manometric[42,43,46] techniques. Gravimetric measurements, however, provide only the total weight change of a sample as a result of sorption, while volumetric/manometric techniques typically involve measuring only the total pressure change in a system of known volume. Neither total sample weight nor the total system pressure change can determine the amount of each individual component sorbed by the sample. The challenge is in determining the sorbed phase composition□at a specified gas phase composition□in addition to the total amount sorbed.

Traditional methods for determining full multicomponent sorption equilibria include closed and open volumetric systems and related variants that use the gravimetric technique. In

https://doi.org/10.1021/acs.iecr.2c00497
Ind. Eng. Chem. Res. 2022, 61, 9774−9784

closed volumetric systems, a known gas mixture is circulated through a sorbent bed. Once equilibrium has been achieved, the gas phase composition is analyzed to allow calculation of the amount of each component sorbed at the final total pressure, P, which is measured but cannot be controlled. Closed gravimetric systems are similar, but the total mass adsorbed is measured using a microbalance. An alternative is open volumetric measurement in which a known gas mixture is flowed through a column and the total outlet flow rate and composition measured.[6] Each approach has advantages and disadvantages.

2.2. The Integral Mass Balance (IMB) Method. The new IMB method is based on an open (flowing) volumetric system. It was described in detail by Broom et al.,[11] so only a summary will be presented here. In a conventional open volumetric experiment, the total inlet molar flow rate and gas mixture compositions are controlled, and the total outlet molar flow rate and outlet compositions determined. The amount of each component i adsorbed can then be calculated, following a step change in the inlet conditions, using the following molar balance expression,

$$\Delta n_i^{\text{ads}} = \int_0^t (f^{in} y_i^{\text{in}} - f^{\text{out}} y_i^{\text{out}})\mathrm{d}t - \Delta n_i^{\text{gas}} \quad (1)$$

where Δn_i^{ads} is the molar adsorbed quantity of component i, f^{in} and f^{out} are the total inlet and outlet molar flow rates, y_i^{in} and y_i^{out} are the inlet and outlet molar concentrations of component i, and Δn_i^{gas} is the molar amount of component i accumulated in the gas phase. This measurement type is relatively quick, but its accuracy is limited by the difficulty in accurately measuring the total outlet flow rate of a gas mixture of changing composition. The IMB method avoids this problem by measuring the weight change of the sample in situ, using a microbalance and the reactor shown in Figure 2.

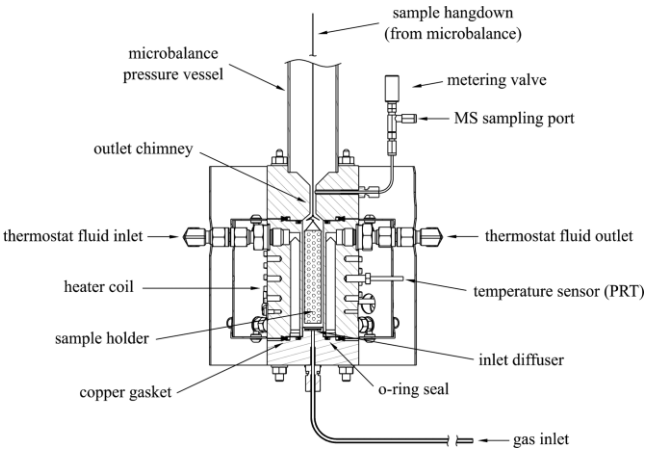

Figure 2. Hiden IMB reactor, key components as shown in Broom et al.[11]

All variables are converted to mass, rather than molar, quantities, allowing the substitution of $F^{\text{out}} = F^{\text{in}} - \mathrm{d}m/\mathrm{d}t$ into the mass balance equivalent of eq 1, where F^{in} and F^{out} are the total inlet and outlet mass flow rates, and $\mathrm{d}m/\mathrm{d}t$ is mass change as a function of time. This gives,

$$\Delta m_i = F^{\text{in}} \int_0^t (Y_i^{\text{in}} - Y_i^{\text{out}})\mathrm{d}t + \int_0^t Y_i^{\text{out}}\mathrm{d}m \quad (2)$$

where Y_i^{in} and Y_i^{out} are the inlet and outlet mass (rather than molar) concentrations of component i, and Δm_i is the mass of component i in the control volume. The need to measure F^{out}, the key source of uncertainty in open volumetric measurements, is thus eliminated. Further consideration of the corrections required to determine the adsorbed quantity yields,[11]

$$M_i \Delta n_i^{\text{ads}} = F^{\text{in}} \int_0^t (Y_i^{\text{in}} - Y_i^{\text{out}})\mathrm{d}t + \int_0^t Y_i^{\text{out}}\mathrm{d}w + \frac{PV^{\text{tot}}}{ZRT}\int_0^t Y_i^{\text{out}}\mathrm{d}\bar{M} - M_i \Delta y_i \frac{PV^{\text{gas}}}{ZRT} \quad (3)$$

where M_i is the molar mass of component i, w is the measured weight of the sample, P is pressure, V^{tot} is the total volume of the system, Z is the compressibility factor of the gas mixture, R is the universal gas constant, T is temperature, $\bar{M}$ is the mean molar mass of the mixture, and V^{gas} is the volume of the gas phase.

The IMB method allows multipoint measurements of multicomponent sorption equilibria to be made quickly, along a defined path, with higher accuracy than open volumetric measurements. Accuracy comparable to closed volumetric measurements is achievable in a fraction of the time. Crucially, the weight of the sample in the pure gas is measured in situ at the start of a binary or multicomponent sorption isotherm measurement, allowing the thermodynamic consistency of data to be checked directly, by comparison to separate pure component measurements; while the measurement along a defined path ends at the other extremity, providing a further consistency check. This is a significant advantage of the IMB method, compared to both open and closed volumetric measurements, which typically determine only single, isolated points at one value of P, T, and y_i. The direction of the measurement can also be reversed, to demonstrate the reversibility of the sorption process.

The method was demonstrated and validated by performing binary O_2/N_2 adsorption measurements on a commercial 5A zeolite (Tosoh 5A) at ambient temperature (296.5 K) and a total pressure of 0.915 MPa.[11] Excellent agreement with previously published data[47] was found, using a 3.5 g sample, with a measurement time of only 4 h for a 20-point isotherm (see Supporting Information (SI) Figure S1). In contrast, other techniques of equivalent accuracy would require approximately 20 days of experimental effort to collect a comparable amount of data. Equilibrium binary N_2/O_2 adsorption isotherms agreed with previously published results (see SI Figure S2) and were used to calculate selectivity as a function of O_2 concentration. In addition to being fast and accurate, the final equilibrium conditions in the gas phase, in terms of T, P, and y_i, can be controlled exactly; the approach to equilibrium at each isotherm point can be monitored using the microbalance and outlet gas composition signals, allowing measurement time to be optimized; and the mass spectrometer signal can be calibrated in situ, which is not the case in the closed volumetric or gravimetric techniques. While binary adsorption has been used so far to validate the technique, eqs 2 and 3 are general, and the method can, in principle, be applied to gas sorption for ternary or higher mixtures. Broom et al.[11] discussed some of the potential limitations of the IMB method, which include the inherent uncertainty in $\bar{M}$, possible problems with buoyancy corrections at elevated total pressures, and difficulties associated with slow sorption kinetics. Inherent uncertainty in $\bar{M}$ is likely to cause more problems when

https://doi.org/10.1021/acs.iecr.2c00497
Ind. Eng. Chem. Res. 2022, 61, 9774−9784

Table 1. Ionic Liquid Physical Properties[49−55]

ionic liquid	formula	MW	melting point	density	viscosity
		g·mol^{-1}	K	kg·m^{-3}	Pa·s
[C_4C_1im][BF_4]	$C_8H_{15}BF_4N_2$	226.03	190.15[52]	1201.17 ± 0.16[54]	0.101 ± 0.003[54]
[C_4C_1im][PF_6]	$C_8H_{15}PF_6N_2$	284.19	265.15[51]	1367.6 ± 0.7[53]	0.271 ± 0.021[55]

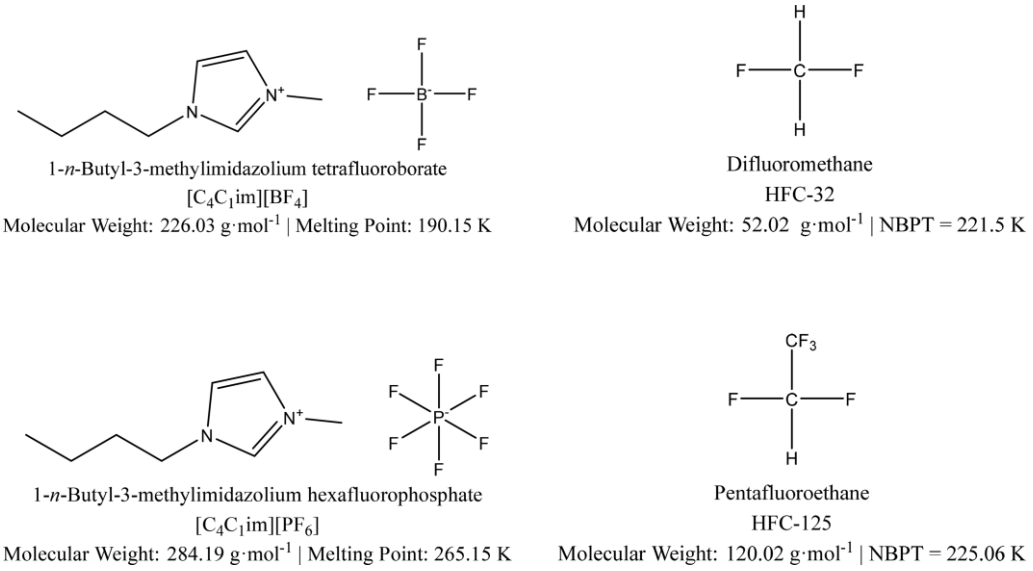

Figure 3. Chemical structures, acronyms, and physical properties of the ILs and HFC refrigerants.[48−52]

studying mixtures of gas species with very different molar masses or densities. However, further work will be required to determine the limits of applicability of the technique, and hence define more clearly where any such problems may lie.

3. MATERIALS AND METHODS

3.1. Materials. Refrigerants HFC-32 (difluoromethane, CH_2F_2, CAS No. 75−10−5) and HFC-125 (pentafluoroethane, CHF_2CF_3, CAS No. 354−33−6) were obtained with a minimum purity of 99.9 wt % and were used as received from The Chemours Company (Newark, DE). The following ILs were purchased from Fluka Chemika (Switzerland): 1-*n*-butyl-3-methylimidazolium tetrafluoroborate ([C_4C_1im][BF_4], assay ≥97 wt %, CAS No. 174501−65−6, Lot and Filling Code No. 1116280 23404335) and 1-*n*-butyl-3-methylimidazolium hexafluorophosphate ([C_4C_1im][PF_6], assay ≥98.6%, CAS No. 174501−64−5, Lot and Filling Code No. 1242554 304070904). The chemical structure and physical properties for the refrigerants and ILs are provided in Table 1 and Figure 3. The National Institute of Standards and Technology (NIST) REFPROP V.10.0 database was used to obtain the liquid and vapor phase densities for HFC-32 and HFC-125.[48] NIST ILTHERMO V.2.0 database #147 and literature were used to obtain IL densities, viscosities, and molecular weights.[49−55]

3.2. Experimental Methodology. The multicomponent gas absorption measurements were made using the first of their kind IGA and XEMIS gas sorption analyzers, with specially designed reactors required for the IMB method (Hiden Isochema Ltd., Warrington, United Kingdom). Both microbalances have a total capacity of 5 g, while the IGA and XEMIS have dynamic weighing ranges of 1 g and 290 mg, respectively, and long-term stabilities of ±1 μg and ±5 μg.

Prior to each experiment, a unique IL sample was prepared. Different containment methods were tested, in order to achieve the best contact with the gas flow in a dynamic system, including supporting the ILs in quartz wool, stainless steel and Al mesh, and tissue paper. Use of quartz wool resulted in slow sorption kinetics in preliminary test measurements, due to poor gas contact, while the mesh provided a low fluid-to-support mass ratio, which can be an issue for gravimetric measurements using microbalances with limited total capacity. Tissue paper, however, provided acceptable kinetics and higher fluid-to-support mass ratios, and so was selected for the subsequent IMB method measurements.

First, a piece of double lined tissue paper was roughly cut to size (8.5 cm × 13.5 cm) and weighed. The IL was then carefully painted onto the paper and then the paper/IL sample was rolled into a cylinder exposing as much surface area as possible. Next, the sample was weighed before being secured in a metal frame. Figure 4 shows an example of a sample that was prepared and loaded into the XEMIS with the IMB method. The IL sample was dried and degassed with a constant flow of helium at room temperature for a minimum of 12 h or until the mass stabilized. This ensured that any trace amount of volatile components (e.g., water) were removed from the sample prior to the experiment. The sample can also be evacuated and heated if required during this pretreatment step. The counterweight can also be adjusted if necessary to account for the weight lost during the degassing process.

The gas sorption experiments were operated in "dynamic mode" with a constant flow of gas over the sample at a fixed *T* and *P* while the inlet gas composition was varied. A GC (gas chromatography) switching valve was used to prepare the gas mixture for introduction into the IMB reactor as shown in the process and instrumentation diagram (P&ID) in SI Figure S3. The gas mixture flows through a bypass line before being

https://doi.org/10.1021/acs.iecr.2c00497
Ind. Eng. Chem. Res. 2022, 61, 9774−9784

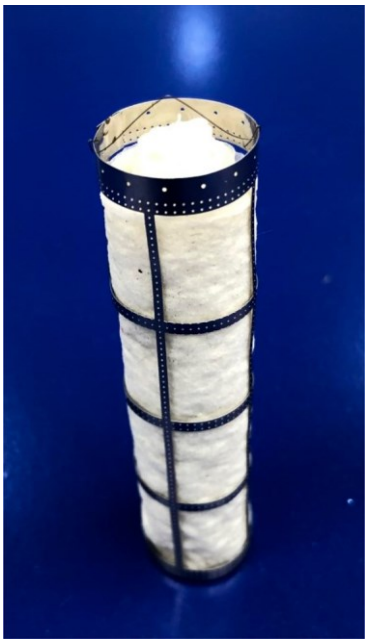

Figure 4. Paper painted with ionic liquid that is then rolled and secured into the metal frame.

switched into the IMB reactor. A time lag must be applied to the mass spectrometer (MS) signal, and this is determined by directly connecting the MS sampling capillary to the inlet where it enters the IMB reactor (see Broom et al.[11] for further details). For the experiments described here, the time lag was typically in the range 25−30 s. Each composition set point was allowed to reach equilibrium until steady state conditions were achieved. Steady state conditions are defined by when the outlet composition of each component, i, equals the inlet composition ($Y_i^{in} = Y_i^{out}$), and when the weight signal, w, from the microbalance is no longer changing ($dw/dt = 0$), see eq 3.

All parameters, including the outlet gas composition and microbalance signal, were recorded using the HISorp software. The temperature was measured with a Pt100 platinum resistance thermometer (PRT) probe with an uncertainty of 0.1 K. Brooks Instruments 5850E mass flow controllers (Hatfield, PA) were used to control the gas flow rates with a maximum flow of 100 mL·min^{-1} and a manufacturer measurement accuracy of ±1% full scale. The flow calibration was further improved by cubic polynomial expansion of the calculated volume flow rate during free pressurization for a series of command values.[11] The total pressure was measured using a GE Sensing PDCR 4020 strain gauge sensor with a measurement accuracy of ±0.04% full scale and a typical control regulation accuracy of ±1 mbar. The outlet stream composition was measured by sampling gas at the exit of the reactor, just above the sample (see Figure 2), using a Hiden Analytical (Warrington, UK) Dynamic Sampling Mass Spectrometer (DSMS).

4. RESULTS AND DISCUSSION

4.1. Binary HFC-32 and HFC-125 Absorption. Binary absorption of HFC-32 and HFC-125 was investigated with [C_4C_1im][BF_4] and [C_4C_1im][PF_6] in the new XEMIS and IGA gravimetric microbalances with the IMB method, respectively. Isothermal vapor liquid equilibrium (VLE) data were measured at five inlet concentrations of HFC-32/HFC-125 (e.g., 1.00/0.00, 0.75/0.25, 0.50/0.50, 0.25/0.75, 0.00/1.00 mole fraction).

The total absorption into the IL and the partial absorption (i.e., individual components) of both HFC-32 and HFC-125 in [C_4C_1im][BF_4] at each inlet concentration (mole fraction) is shown in Table 2 and Figure 5 (see SI Table S1 and Figure S6 for mmol/g and SI Table S2 for mass fraction). As expected, when the inlet concentration of HFC-32 decreases, the absorption of HFC-32 in [C_4C_1im][BF_4] decreases. As the inlet concentration of HFC-125 increases, the absorption of HFC-125 in [C_4C_1im][BF_4] increases. However, as the inlet concentration of HFC-125 increases and HFC-32 decreases, the total absorption in the IL decreases. This agrees with literature data that consistently shows that HFC-32 has higher solubility in fluorinated ILs than HFC-125.[17] HFC-32 and HFC-125 have nearly equal absorption (e.g., 0.05 mole fraction) at the inlet concentration of 0.75 HFC-125 and 0.25 HFC-32 mole fractions.

Table 2. Experimental VLE in Terms of Mole Percent for HFC-32/HFC-125/[C_4C_1im][BF_4] Mixtures at 298.15 K Using XEMIS + IMB

HFC-32 (1) + HFC-125 (2) + [C_4C_1im][BF_4] (3)				
T = 298.15 K | P = 0.25 MPa | flow rate = 6.25 mL·min^{-1}				
HFC-125 inlet (mol %)	HFC-32 inlet (mol %)	total absorption (mol %)	HFC-125 absorption (mol %)	HFC-32 absorption (mol %)
0	100	17.2	0.0 ± <0.01	17.2 ± 0.05
25	75	14.7	1.8 ± 0.12	13.4 ± 0.14
50	50	12.1	3.3 ± 0.23	9.4 ± 0.23
75	25	9.3	4.9 ± 0.34	4.8 ± 0.33
100	0	6.5	6.5 ± 0.46	0.0 ± 0.43

The mixture absorption of HFC-32 and HFC-125 in [C_4C_1im][PF_6] at two different pressures and flow rates are shown in Table 3 and Figure 6 (see SI Table S3 and Figure S7 for mmol/g and SI Table S4 for mass fraction). The total absorption at 0.1 MPa is lower than the absorption at 0.25 MPa; therefore, absorption increases as pressure increases, as expected. One interesting trend when comparing plots (a) and (b) in Figures 5 and 6, is how the total absorption changes as a function of inlet concentration when the differences in molecular weight for HFC-32 and HFC-125 are taken into account ($MW_{HFC\text{-}32}$ = 52.024 g·mol^{-1} and $MW_{HFC\text{-}125}$ = 120.02 g·mol^{-1}). The difference in solubility of HFC-32 and HFC-125 is larger in terms of mole fraction than mass fraction in both [C_4C_1im][BF_4] and [C_4C_1im][PF_6]. The same trend can be seen in the VLE measurements by Morais et al.[17] (see SI Tables S5 and S6). The relative difference in solubility between HFC-32 and HFC-125 is an important factor to consider when designing a separation process, especially in terms of mass fraction.

The experimental solubility data for HFC-32/HFC-125 in [C_4C_1im][BF_4] and [C_4C_1im][PF_6] at 298.15 K are provided in Tables 2 and 3, respectively. The solubility data, in terms of moles per gram and mass percent, are presented in SI Tables S1−S4.

The mixture absorption of HFC-32 and HFC-125 in [C_4C_1im][BF_4] and [C_4C_1im][PF_6] at 298.15 K, 0.25 MPa, and 6.25 mL·min^{-1} are compared in Figure 7. HFC-125 shows nearly identical absorption in both [C_4C_1im][BF_4] and [C_4C_1im][PF_6] until the inlet feed is nearly 1.0 mole fraction

https://doi.org/10.1021/acs.iecr.2c00497
Ind. Eng. Chem. Res. 2022, 61, 9774−9784

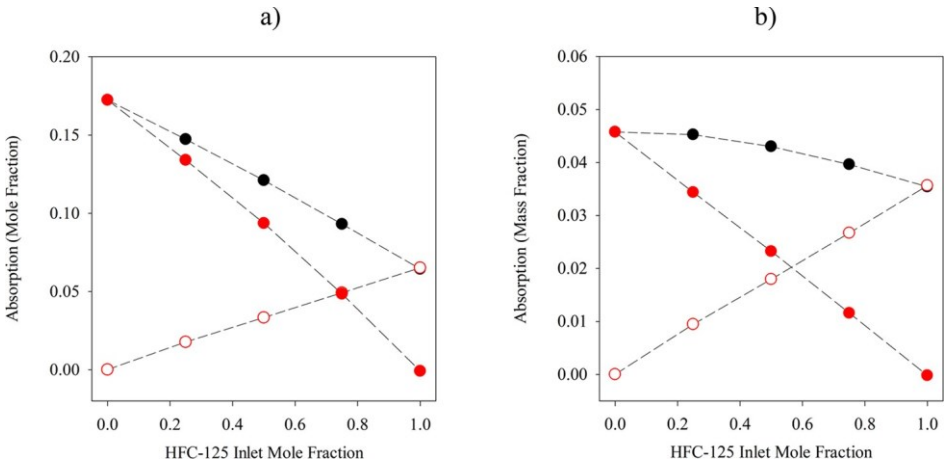

Figure 5. (a) Equilibrium binary absorption in terms of mole fraction. b) Equilibrium binary absorption in terms of mass fraction. Total absorption (solid black circles), partial absorption of HFC-32 (solid red circles), and partial absorption of HFC-125 (open red circles) at 298.15 K, 0.25 MPa, and 6.25 ml·min^{-1} in [C_4C_1im][BF_4]. Dashed lines are guides for the reader.

Table 3. Experimental VLE in Terms of Mole Percent for HFC-32/HFC-125/[C_4C_1im][PF_6] Mixtures at 298.15 K Using IGA + IMB

HFC-32 (1) + HFC-125 (2) + [C_4C_1im][PF_6] (3)				
HFC-125 inlet (mol %)	HFC-32 inlet (mol %)	total absorption (mol %)	HFC-125 absorption (mol %)	HFC-32 absorption (mol %)
T = 298.15 K | P = 0.1 MPa | flow rate = 12.5 mL·min^{-1}				
0	100	8.8	0.0 ± < 0.01	8.8 ± 0.02
25	75	7.4	0.6 ± 0.03	6.8 ± 0.04
50	50	5.8	1.3 ± 0.05	4.6 ± 0.06
75	25	4.2	2.0 ± 0.08	2.3 ± 0.07
100	0	2.7	2.7 ± 0.11	0.0 ± 0.08
T = 298.15 K | P = 0.25 MPa | flow rate = 6.25 mL·min^{-1}				
0	100	19.8	0.0 ± 0.01	19.8 ± 0.03
25	75	16.9	1.8 ± 0.05	15.7 ± 0.07
50	50	13.9	3.5 ± 0.10	11.2 ± 0.10
75	25	10.9	5.0 ± 0.15	6.5 ± 0.14
100	0	7.2	7.2 ± 0.21	0.0 ± 0.18

HFC-125, at which point the HFC-125 has slightly higher sorption in [C_4C_1im][PF_6]. HFC-32 absorption was consistently higher in [C_4C_1im][PF_6], which also translated to the total mixture absorption. The difference in total absorption for [C_4C_1im][BF_4] and [C_4C_1im][PF_6] is therefore determined by the solubility of HFC-32 in each of the ILs and the solubility difference of HFC-125 had a minimal impact.

The m, T, P, and F as a function of t for HFC-32 and HFC-125 with [C_4C_1im][BF_4] at 298.15 K, 0.25 MPa, and 6.25 mL·min^{-1} is shown in SI Figures S4 and S5.

4.3. Comparison of Binary Absorption and Single-Component Absorption of HFC-32 and HFC-125 in [C_4C_1im][BF_4]. The pure component HFC-32 and HFC-125 absorption data for [C_4C_1im][BF_4] using the XEMIS gravimetric microbalance with IMB method was compared to the IGA gravimetric data for [C_4C_1im][BF_4] from Morais et al.[17] At constant temperature and pressure, the total amount absorbed at the composition end points for the mixture data (pure HFC-32 or HFC-125) must equal the single component

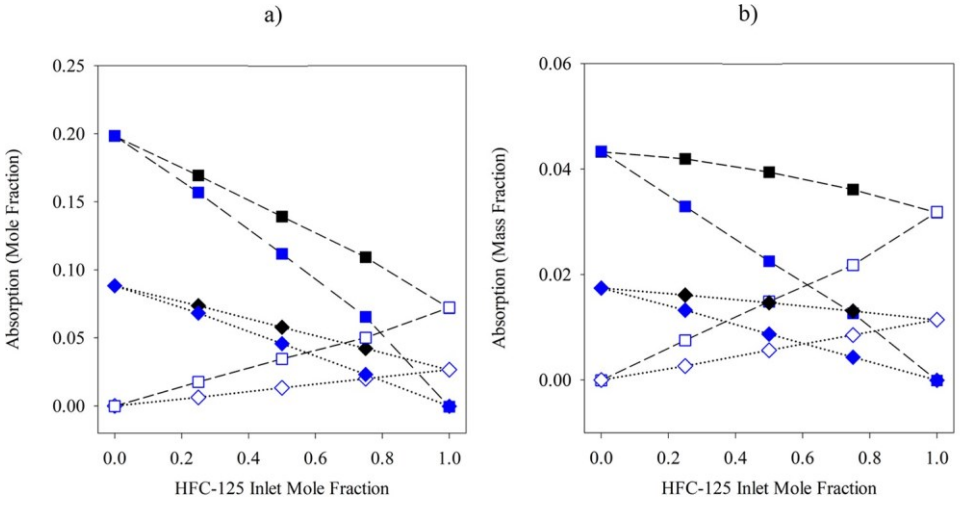

Figure 6. (a) Equilibrium binary absorption in terms of mole fraction. b) Equilibrium binary absorption in terms of mass fraction. Total absorption (solid black diamond), partial absorption of HFC-32 (solid blue diamond), and partial absorption of HFC-125 (open blue diamond) at 298.15 K, 0.1 MPa, and 12.5 ml·min^{-1} in [C_4C_1im][PF_6]. Total absorption (solid black square), partial absorption of HFC-32 (solid blue square), and partial absorption of HFC-125 (open blue square) at 298.15 K, 0.25 MPa, and 6.25 ml·min^{-1} in [C_4C_1im][PF_6]. Dashed lines are guides for the reader.

https://doi.org/10.1021/acs.iecr.2c00497
Ind. Eng. Chem. Res. 2022, 61, 9774−9784

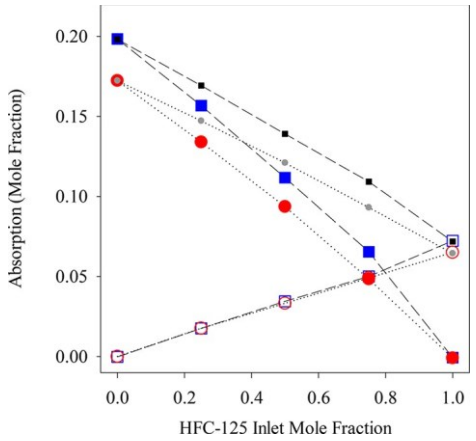

Figure 7. Comparison of mixture absorption in $[C_4C_1im][BF_4]$ and $[C_4C_1im][PF_6]$ at 298.15 K, 0.25 MPa, and 6.25 ml·min^{-1}. Total absorption (solid grey circle), partial absorption of HFC-32 (solid red circle), and partial absorption of HFC-125 (open red circle) in $[C_4C_1im][BF_4]$. Total absorption (solid black square), partial absorption of HFC-32 (solid blue square), and partial absorption of HFC-125 (open blue square) in $[C_4C_1im][PF_6]$.

sorption.[56] This is an important test of the thermodynamic consistency of mixture sorption data and increases confidence in the accuracy of the data (see Shade et al.[56] and Talu and Myers[57] for examples). The experimental VLE data reported by Morais et al.[17] for HFC-32/$[C_4C_1im][BF_4]$ and HFC-125/$[C_4C_1im][BF_4]$ at 298.15 K is presented in SI Table S5.

The IMB method measurements begin with an inlet concentration of pure HFC-32, which is in good agreement (i.e., 0.02 absolute difference in mole fraction) with the pure component IGA data of Morais et al.[17] at the same T and P. The isotherm shown in Figure 8 for the pure component IGA data was fit using the van der Waals EoS model.[17] Next, the IMB method decreases the HFC-32 inlet concentration, while increasing the HFC-125 concentration, and measures the

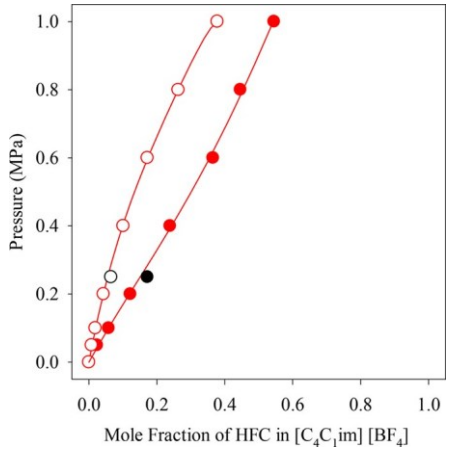

Figure 8. Comparison of IGA VLE and XEMIS with IMB VLE (mole fraction) for HFC-32 and HFC-125 in $[C_4C_1im][BF_4]$. Symbols are measured experimental data, solid lines are van der Waals EoS model predictions, and dashed lines are guides for the reader. IGA data: HFC-32 (solid red circle) and HFC-125 (open red circle) in $[C_4C_1im][BF_4]$ at 298.15 K. XEMIS with IMB data: HFC-32 (solid black circle) and HFC-125 (open black circle) in $[C_4C_1im][BF_4]$ at 298.15 K, 0.25 MPa, and 6.25 ml·min^{-1}. IGA data and van der Waals EoS model predictions for $[C_4C_1im][BF_4]$ reported by Morais et al.[17]

equilibrium sorption at discrete inlet compositions (e.g., 0.75/0.25, 0.50/0.50, and 0.25/0.75 mole fraction HFC-32/HFC-125) until it reaches pure HFC-125. For this reason, comparing the pure HFC-125 results with the XEMIS IMB method is a significantly different process than comparing the pure HFC-125 results with the IGA method. Interestingly, the pure HFC-125 sorption using the XEMIS IMB method is also in good agreement (i.e., 0.01 absolute difference in mole fraction) with the pure component IGA data at the same T and P, see Table 4. This result confirms that the HFC-32 that

Table 4. Absolute Difference Between the IGA and XEMIS + IMB Data at 298.15 K for HFC-32/$[C_4C_1im][BF_4]$ and HFC-125/$[C_4C_1im][BF_4]$. IGA Data from Morais et al.[17]

HFC-32 (1) + $[C_4C_1im][BF_4]$ (2)			
P (MPa)	IGA (mol frac)	XEMIS + IMB (mol frac)	absolute difference
0.25	0.15	0.17	0.02
HFC-125 (1) + $[C_4C_1im][BF_4]$ (2)			
P (MPa)	IGA (mol frac)	XEMIS + IMB (mol frac)	absolute difference
0.25	0.06	0.07	0.01

absorbs in the IL also desorbs via physical sorption by the displacement with HFC-125, resulting in no difference between the XEMIS IMB and pure component IGA methods. This is an important finding that has not been previously reported for HFCs in $[C_4C_1im][BF_4]$.

4.4. Comparison of Binary Absorption and Single-Component Absorption of HFC-32 and HFC-125 in $[C_4C_1im][PF_6]$. The pure component HFC-32 and HFC-125 absorption data for $[C_4C_1im][PF_6]$ using the IGA gravimetric microbalance with IMB method was compared to the IGA gravimetric data for $[C_4C_1im][PF_6]$ from Morais et al.[17] The experimental VLE data reported by Morais et al. for HFC-32/$[C_4C_1im][PF_6]$ and HFC-125/$[C_4C_1im][PF_6]$ at 298.15 K can be found in SI Table S6.

Similar to the previous results with $[C_4C_1im][BF_4]$, the absorption of pure HFC-32 using the pure component IGA and IGA + IMB methods are in good agreement (i.e., 0.01 absolute difference at 0.1 MPa and 0.02 absolute difference at 0.25 MPa in mole faction) at the same T and P, as shown in Table 5 and Figure 9. Furthermore, the HFC-125 completely displaced the HFC-32 in the $[C_4C_1im][PF_6]$, which again supports a physical sorption process, and the pure HFC-125 sorption was in good agreement between the pure component IGA and IGA + IMB methods (i.e., < 0.01 absolute difference at 0.1 MPa and 0.01 absolute difference at 0.25 MPa in mole fraction) at the same T and P, as shown in Table 5. Again, this

Table 5. Absolute Difference between the IGA and IGA + IMB Data at 298.15 K for HFC-32/$[C_4C_1im][PF_6]$ and HFC-125/$[C_4C_1im][PF_6]$. IGA Data from Morais et al.[17]

HFC-32 (1) + $[C_4C_1im][PF_6]$ (2)			
P (MPa)	IGA (mol frac)	IGA + IMB (mol frac)	absolute difference
0.1	0.08	0.09	0.01
0.25	0.18	0.20	0.02
HFC-125 (1) + $[C_4C_1im][PF_6]$ (2)			
P (MPa)	IGA (mol frac)	IGA + IMB (mol frac)	absolute difference
0.1	0.02	0.03	0.01
0.25	0.06	0.07	0.01

https://doi.org/10.1021/acs.iecr.2c00497
Ind. Eng. Chem. Res. 2022, 61, 9774−9784

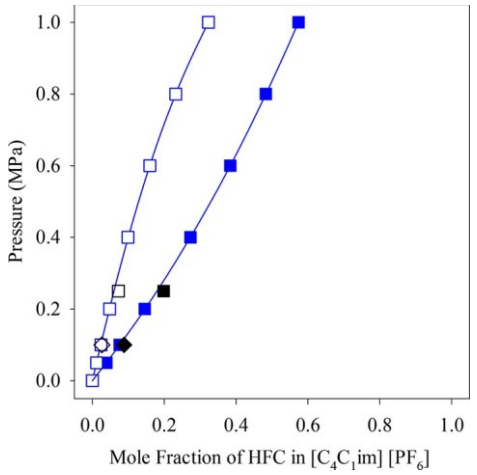

Figure 9. Comparison of IGA VLE and IGA with IMB VLE (mole fraction) for HFC-32 and HFC-125 in [C_4C_1im][PF_6]. Symbols are measured experimental data, solid lines are van der Waals EoS model predictions, and dashed lines are guides for the reader. IGA data: HFC-32 (solid blue square) and HFC-125 (open blue square) in [C_4C_1im][PF_6] at 298.15 K. IGA with IMB data: HFC-32 (solid black diamond) and HFC-125 (open black diamond) in [C_4C_1im]-[PF_6] at 298.15 K, 0.1 MPa, and 12.5 ml·min^{-1} and HFC-32 (solid black square) and HFC-125 (open black square) in in [C_4C_1im][PF_6] at 298.15 K, 0.25 MPa, and 6.25 ml·min^{-1}. IGA data and van der Waals EoS model predictions for [C_4C_1im][PF_6] reported by Morais et al.[17]

is an important finding that has not been previously reported for HFCs in [C_4C_1im][PF_6].

4.5. Selectivity. The equilibrium selectivity for HFC-32 was calculated in the HISorp software for each of the mixture compositions investigated for both [C_4C_1im][BF_4] and [C_4C_1im][PF_6]. The following equation was used:[11]

$$S_{eq} = \left(\frac{n_i / y_i}{n_j / y_j} \right)_{T,P} \quad (4)$$

where n_i and n_j are the partial molar absorption of HFC (i = HFC-32 and j = HFC-125) and y_i and y_j are their mole fractions in the gas phase.[11] The equilibrium selectivity for HFC-32 as a function of the inlet gas composition for [C_4C_1im][BF_4] at 298.15 K, 0.25 MPa, and 6.25 mL·min^{-1} is shown in Table 6. There was no statistical difference in the HFC-32 selectivity as the inlet HFC-125 concentration increases from 0.25 to 0.75 mole fraction, as shown in Figure 10. The uncertainty in selectivities shown in Figure 10 was derived from the uncertainty on equilibrium readings from the calculated accumulation due to all known factors including manufacturers data and respective calibration certificates, as reported by Broom et al.[11]

Table 6. HFC-32 Selectivity from Mixture Absorption in [C_4C_1im][BF_4] at 298.15 K, 0.25 MPa, and 6.25 mL·min^{-1} using XEMIS + IMB

HFC-32 (1) + HFC-125 (2) + [C_4C_1im][BF_4] (3)		
T = 298.15 K | P = 0.25 MPa | flow rate = 6.25 mL·min^{-1}		
HFC-125 inlet (mol %)	HFC-32 inlet (mol %)	HFC-32 selectivity
25	75	2.86 ± 0.20
50	50	3.00 ± 0.21
75	25	2.95 ± 0.27

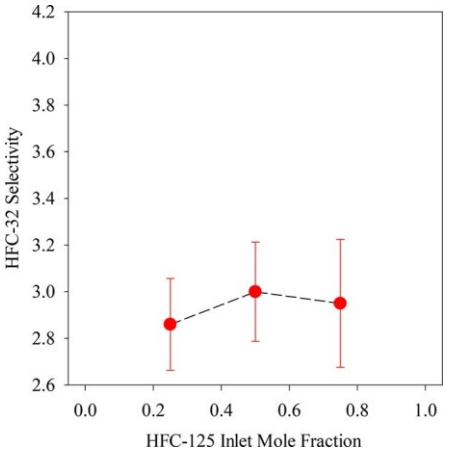

Figure 10. HFC-32 Selectivity with error bars from mixture absorption in [C_4C_1im][BF_4] at 298.15 K, 0.25 MPa, and 6.25 mL·min^{-1}.

The selectivity for HFC-32 at 298.15 K, as a function of the inlet gas composition, for [C_4C_1im][PF_6] at 0.10 MPa and 12.5 mL·min^{-1}, and at 0.25 MPa and 6.25 mL·min^{-1}, is shown in Table 7 and Figure 11. Uncertainties were calculated as

Table 7. HFC-32 Selectivity from Mixture Absorption in [C_4C_1im][PF_6] at 298.15 K, 0.25 MPa, and 6.25 mL·min^{-1} Using IGA + IMB

HFC-32 (1) + HFC-125 (2) + [C_4C_1im][PF_6] (3)		
HFC-125 Inlet (mol %)	HFC-32 Inlet (mol %)	HFC-32 selectivity
T = 298.15 K | P = 0.1 MPa | flow rate = 12.5 mL·min^{-1}		
25	75	3.87 ± 0.16
50	50	3.56 ± 0.15
75	25	3.48 ± 0.18
T = 298.15 K | P = 0.25 MPa | flow rate = 6.25 mL·min^{-1}		
25	75	3.45 ± 0.10
50	50	3.51 ± 0.10
75	25	3.98 ± 0.14

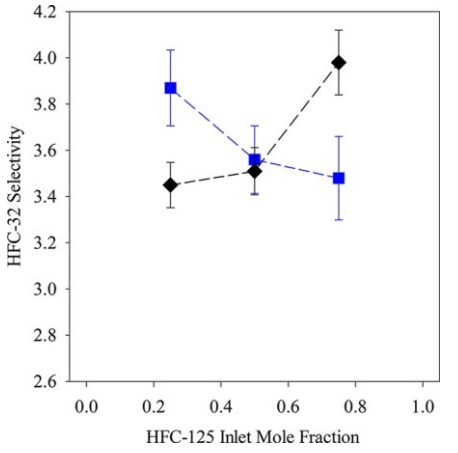

Figure 11. HFC-32 Selectivity with error bars from mixture absorption in [C_4C_1im][PF_6] at 298.15 K with one set at 0.1 MPa and 12.5 ml·min^{-1} (solid black diamond) and one at 0.25 MPa and 6.25 ml·min^{-1} (solid blue square).

https://doi.org/10.1021/acs.iecr.2c00497
Ind. Eng. Chem. Res. 2022, 61, 9774−9784

described above. In this case, the HFC-32 selectivity increased at 0.1 MPa and decreased at 0.25 MPa as a function of increasing HFC-125 inlet concentration, but it was within statistical uncertainty at a composition of y = 0.5/0.5 HFC-32/HFC-125 for both pressures. In addition, the HFC-32 selectivity was 35%, 19%, and 18% higher in [C_4C_1im][PF_6] compared with [C_4C_1im][BF_4] at 0.1 MPa and y = 0.25, 0.50, and 0.75 mole fraction HFC-125, respectively.

5. CONCLUSIONS

Studying the multicomponent absorption of gases into liquids in an efficient and accurate manner has been an ongoing challenge for researchers, resulting in most of the modeling relying on single component absorption data. The IGA and XEMIS gravimetric microbalances with IMB method will change this paradigm and this work presents the first binary absorption measurements of HFC-32 and HFC-125 with [C_4C_1im][BF_4] and [C_4C_1im][PF_6]. The total and partial sorption of HFC-32 and HFC-125 as a function of inlet composition were measured at 298.15 K, with pressures ranging from 0.1 to 0.25 MPa and flow rates ranging from 6.25 mL·min^{-1} to 12.5 mL·min^{-1}. Three key conclusions can be drawn from these experiments: (1) the difference in total absorption for [C_4C_1im][BF_4] and [C_4C_1im][PF_6] was determined by the solubility of HFC-32 in each of the ILs and the solubility difference of HFC-125 had only a minimal impact; (2) the HFC-32 that absorbs in [C_4C_1im][BF_4] and [C_4C_1im][PF_6] desorbs via physical sorption by the displacement with HFC-125, which was validated by comparison of the IGA + IMB and XEMIS + IMB methods with the IGA method using single gases; and (3) the HFC-32 equilibrium selectivity for [C_4C_1im][PF_6] compared with [C_4C_1im][BF_4] was 18 to 35% higher depending on the inlet HFC-125 composition (y = 0.75 to 0.25). Molecular simulations based on this experimental data are being developed for a future publication. The results of this work are being used to design the first extractive distillation process using an ionic liquid entrainer for separation of azeotropic refrigerant mixtures such as R-410A.

ASSOCIATED CONTENT

Supporting Information

The Supporting Information is available free of charge at https://pubs.acs.org/doi/10.1021/acs.iecr.2c00497.

O_2 + N_2 adsorption for zeolite 5A; P of Hiden Isochema XEMIS; XEMIS with IMB data for m, T, P, and F as a function of t; equilibrium binary absorption plots in mmol/g; Experimental VLE data tables (PDF)

AUTHOR INFORMATION

Corresponding Author

Mark B. Shiflett – *Institute for Sustainable Engineering, Lawrence, Kansas 66045, United States; Department of Chemical and Petroleum Engineering, University of Kansas, Lawrence, Kansas 66045, United States*; orcid.org/0000-0002-8934-6192; Email: mark.b.shiflett@ku.edu

Authors

Kalin R. Baca – *Institute for Sustainable Engineering, Lawrence, Kansas 66045, United States; Department of Chemical and Petroleum Engineering, University of Kansas, Lawrence, Kansas 66045, United States*; orcid.org/0000-0002-7292-8698

Darren P. Broom – *Hiden Isochema Ltd, Warrington, United Kingdom WA5 7TS*; orcid.org/0000-0002-1328-7376

Mark G. Roper – *Hiden Isochema Ltd, Warrington, United Kingdom WA5 7TS*

Michael J. Benham – *Hiden Isochema Ltd, Warrington, United Kingdom WA5 7TS*

Complete contact information is available at: https://pubs.acs.org/10.1021/acs.iecr.2c00497

Notes

The authors declare no competing financial interest.

ACKNOWLEDGMENTS

We thank Dr. Luke Simoni at The Chemours Company for providing the HFC-32 and HFC-125. This material is based upon work supported by the National Science Foundation under Grant No. 1920252.

ABBREVIATIONS:

CFC, chlorofluorocarbon
[C_4C_1im][BF_4], 1-*n*-Butyl-3-methylimidazolium tetrafluoroborate
[C_4C_1im][PF_6], 1-*n*-Butyl-3-methylimidazolium hexafluorophosphate
F, Flow
GWP, global warming potential
HFC, hydrofluorocarbon
HCFC, hydrochlorofluorocarbon
HFC-125, pentafluoroethane, CHF_2CF_3
HFC-32, difluoromethane, CH_2F_2
HFO, hydrofluoroolefin
IL, ionic liquid
m, mass
ODP, ozone depletion potential
P, pressure
T, temperature
t, time

REFERENCES

(1) Cai, X.; Gharagheizi, F.; Bingel, L. W.; Shade, D.; Walton, K. S.; Sholl, D. S. A Collection of More than 900 Gas Mixture Adsorption Experiments in Porous Materials from Literature Meta-Analysis. *Ind. Eng. Chem. Res.* 2021, *60* (1), 639−651.

(2) Broom, D. P.; Thomas, K. M. Gas Adsorption by Nanoporous Materials: Future Applications and Experimental Challenges. *MRS Bull.* 2013, *38* (5), 412−421.

(3) Fletcher, A. J.; Benham, M. J.; Thomas, K. M. Multicomponent Vapor Sorption on Active Carbon by Combined Microgravimetry and Dynamic Sampling Mass Spectrometry. *J. Phys. Chem. B* 2002, *106* (30), 7474−7482.

(4) Broom, D. P. Characterizing Adsorbents for Gas Separations. *Chem. Eng. Prog.* 2018, 30−37.

(5) Broom, D. P. Bridging the Gap: Gas Adsorption − from the R&D Lab to Industry. *The Chemical Engineer* 2017, 36−38.

(6) Talu, O. Needs, Status, Techniques and Problems with Binary Gas Adsorption Experiments. *Adv. Colloid Interface Sci.* 1998, *76−77*, 227−269.

(7) Sircar, S.; Myers, A. L. Gas Separation in Zeolites. In *Handbook of Zeolite Science and Technology*; Auerbach, S. M., Carrado, K. A., Dutta, P. K., Eds.; Marcel Dekker, Inc: New York, 2003; pp 1063−1105.

(8) Ruthven, D. M. *Principles of Adsorption and Adsorption Processes*; Wiley: New York, 1984.
(9) Yang, R. T. *Gas Separation by Adsorption Processes*; Imperial College Press: London, 1997.
(10) *NIST Workshop Summary Report, Measurement Needs in the Adsorption Sciences*, 2015.
(11) Broom, D. P.; Talu, O.; Benham, M. J. Integral Mass Balance (IMB) Method for Measuring Multicomponent Gas Adsorption Equilibria in Nanoporous Materials. *Ind. Eng. Chem. Res.* 2020, *59* (46), 20478−20491.
(12) Arora, P.; Seshadri, G.; Tyagi, A. K. Fourth-Generation Refrigerant: HFO 1234yf. *Curr. Sci.* 2018, *115* (8), 1497−1503.
(13) McLinden, M. O.; Huber, M. L. (R)Evolution of Refrigerants. *J. Chem. Eng. Data* 2020, *65* (9), 4176−4193.
(14) US EPA. AIM Act https://www.epa.gov/climate-hfcs-reduction/aim-act (accessed 2021 −08 −06).
(15) US EPA. Proposed Rule - Phasedown of Hydrofluorocarbons: Establishing the Allowance Allocation and Trading Program under the AIM Act https://www.epa.gov/climate-hfcs-reduction/proposed-rule-phasedown-hydrofluorocarbons-establishing-allowance-allocation (accessed 2021−08−03).
(16) Baca, K. R.; Olsen, G. M.; Matamoros Valenciano, L.; Bennett, M. G.; Haggard, D. M.; Befort, B. J.; Garciadiego, A.; Dowling, A. W.; Maginn, E. J.; Shiflett, M. B. Phase Equilibria and Diffusivities of HFC-32 and HFC-125 in Ionic Liquids for the Separation of R-410A. *ACS Sustainable Chem. Eng.* 2022, *10* (2), 816−830.
(17) Morais, A. R. C.; Harders, A. N.; Baca, K. R.; Olsen, G. M.; Befort, B. J.; Dowling, A. W.; Maginn, E. J.; Shiflett, M. B. Phase Equilibria, Diffusivities, and Equation of State Modeling of HFC-32 and HFC-125 in Imidazolium-Based Ionic Liquids for the Separation of R-410A. *Ind. Eng. Chem. Res.* 2020, *59* (40), 18222−18235.
(18) Minnick, D. L.; Shiflett, M. B. Solubility and Diffusivity of Bromodifluoromethane (Halon-1201) in Imidazolium Ionic Liquids: $[C_2C_1im][Tf_2N]$, $[C_4C_1im][BF_4]$, and $[C_4C_1im][PF_6]$. *J. Chem. Eng. Data* 2020, *65* (7), 3277−3286.
(19) Minnick, D. L.; Shiflett, M. B. Solubility and Diffusivity of Chlorodifluoromethane in Imidazolium Ionic Liquids: [Emim]-[Tf_2N], [Bmim][BF_4], [Bmim][PF_6], and [Emim][TFES]. *Ind. Eng. Chem. Res.* 2019, *58* (25), 11072−11081.
(20) Turnaoglu, T.; Shiflett, M. B. 110th Anniversary: The First Thermodynamic and Kinetic Analysis of Ammonia in Imidazolium-Based Ionic Liquids Using a Gravimetric Microbalance. *Ind. Eng. Chem. Res.* 2019, *58* (11), 4644−4655.
(21) Minnick, D. L.; Turnaoglu, T.; Rocha, M. A.; Shiflett, M. B. Review Article: Gas and Vapor Sorption Measurements Using Electronic Beam Balances. *J. Vac. Sci. Technol. A: Vacuum, Surfaces, and Films* 2018, *36* (5), 050801.
(22) Shiflett, M. B.; Maginn, E. J. The Solubility of Gases in Ionic Liquids. *AIChE J.* 2017, *63* (11), 4722−4737.
(23) Shiflett, M. B.; Corbin, D. R.; Elliott, B. A.; Subramoney, S.; Kaneko, K.; Yokozeki, A. Sorption of Trifluoromethane in Activated Carbon. *Adsorption* 2014, *20*, 565−575.
(24) Shiflett, M. B.; Maginn, E. J. The Solubility of Gases in Ionic Liquids. In *Ionic Liquids Uncoiled: Critical Expert Overviews*; Plechkova, N. V., Seddon, K. R., Eds.; John Wiley & Sons, 2012; pp 349−386.
(25) Shiflett, M. B.; Corbin, D. R.; Elliott, B. A.; Yokozeki, A. Sorption of Trifluoromethane in Zeolites and Ionic Liquid. *J. Chem. Thermodyn.* 2013, *64*, 40−49.
(26) Shiflett, M. B.; Corbin, D. R.; Yokozeki, A. Comparison of the Sorption of Trifluoromethane (R-23) on Zeolites and in an Ionic Liquid. *Adsorpt. Sci. Technol.* 2013, *31* (1), 59−83.
(27) Shiflett, M. B.; Elliott, B. A.; Lustig, S. R.; Sabesan, S.; Kelkar, M. S.; Yokozeki, A. Phase Behavior of CO_2 in Room-Temperature Ionic Liquid 1-Ethyl-3-Ethylimidazolium Acetate. *ChemPhysChem* 2012, *13* (7), 1806−1817.
(28) Yokozeki, A.; Shiflett, M. B. *Solubility of Fluorocarbons in Room Temperature Ionic Liquids*, ACS Symposium Series; Plechkova, N. V., Rogers, R. D., Seddon, K. R., Eds.; American Chemical Society: Washington DC, 2009; pp 21−42.
(29) Shiflett, M. B.; Yokozeki, A. Binary Vapor-Liquid and Vapor-Liquid-Liquid Equilibria of Hydrofluorocarbons (HFC-125 and HFC-143a) and Hydrofluoroethers (HFE-125 and HFE-143a) with Ionic Liquid [Emim][Tf_2N]. *J. Chem. Eng. Data* 2008, *53* (2), 492−497.
(30) Kumelan, J.; Pérez-Salado Kamps, A.; Tuma, D.; Yokozeki, A.; Shiflett, M. B.; Maurer, G. Solubility of Tetrafluoromethane in the Ionic Liquid [Hmim][Tf_2N]. *J. Phys. Chem. B* 2008, *112* (10), 3040−3047.
(31) Shiflett, M. B.; Yokozeki, A. Solubility Differences of Halocarbon Isomers in Ionic Liquid [Emim][Tf_2N]. *J. Chem. Eng. Data* 2007, *52* (5), 2007−2015.
(32) Yokozeki, A.; Shiflett, M. B. Global Phase Behaviors of Trifluoromethane in Ionic Liquid [Bmim][PF_6]. *AIChE J.* 2006, *52* (11), 3952−3957.
(33) Shiflett, M. B.; Yokozeki, A. Gaseous Absorption of Fluoromethane, Fluoroethane, and 1,1,2,2-Tetrafluoroethane in 1-Butyl-3-Methylimidazolium Hexafluorophosphate. *Ind. Eng. Chem. Res.* 2006, *45* (18), 6375−6382.
(34) Shiflett, M. B.; Harmer, M. A.; Junk, C. P.; Yokozeki, A. Solubility and Diffusivity of 1,1,1,2-Tetrafluoroethane in Room-Temperature Ionic Liquids. *Fluid Phase Equilib.* 2006, *242* (2), 220−232.
(35) Shiflett, M. B.; Harmer, M. A.; Junk, C. P.; Yokozeki, A. Solubility and Diffusivity of Difluoromethane in Room-Temperature Ionic Liquids. *J. Chem. Eng. Data* 2006, *51* (2), 483−495.
(36) Shiflett, M. B.; Yokozeki, A. Solubility and Diffusivity of Hydrofluorocarbons in Room-Temperature Ionic Liquids. *AIChE J.* 2006, *52* (3), 1205−1219.
(37) Sircar, S. Basic Research Needs for Design of Adsorptive Gas Separation Processes. *Ind. Eng. Chem. Res.* 2006, *45* (16), 5435−5448.
(38) Walton, K. S.; Sholl, D. S. Predicting Multicomponent Adsorption: 50 Years of the Ideal Adsorbed Solution Theory. *AIChE J.* 2015, *61* (9), 2757−2762.
(39) Sircar, S. Recent Developments in Macroscopic Measurement of Multicomponent Gas Adsorption Equilibria, Kinetics, and Heats. *Ind. Eng. Chem. Res.* 2007, *46* (10), 2917−2927.
(40) Talu, O. Measurement and Analysis of Mixture Adsorption Equilibrium in Porous Solids. *Chem. Ing. Tech.* 2011, *83* (1−2), 67−82.
(41) Walton, K. S. 110th Anniversary: Commentary: Perspectives on Adsorption of Complex Mixtures. *Ind. Eng. Chem. Res.* 2019, *58* (37), 17100−17105.
(42) Belmabkhout, Y.; Frère, M.; de Weireld, G. High-Pressure Adsorption Measurements. A Comparative Study of the Volumetric and Gravimetric Methods. *Meas. Sci. Technol.* 2004, *15* (5), 848.
(43) Keller, J. U.; Staudt, R. *Gas Adsorption Equilibria: Experimental Methods and Adsorptive Isotherms*; Springer US: New York, 2005.
(44) Benham, M. J.; Ross, D. K. Experimental Determination of Absorption-Desorption Isotherms by Computer-Controlled Gravimetric Analysis. *Z. Phys. Chem.* 1989, *163* (Part_1), 25−32.
(45) de Weireld, G.; Frère, M.; Jadot, R. Automated Determination of High-Temperature and High-Pressure Gas Adsorption Isotherms Using a Magnetic Suspension Balance. *Meas. Sci. Technol.* 1999, *10* (2), 117−126.
(46) Rouquerol, J.; Rouquerol, F.; Llewellyn, P.; Maurin, G.; Sing, K. S. W. *Adsorption by Powders and Porous Solids: Principles, Methodology and Applications*, 2nd ed.; Academic Press: London, 2014 DOI: 10.1016/C2010-0-66232-8.
(47) Talu, O.; Li, J.; Kumar, R.; Mathias, P. M.; Moyer, J. D.; Schork, J. M. Measurement and Analysis of Oxygen/Nitrogen/ 5A-Zeolite Adsorption Equilibria for Air Separation. *Gas Sep. Purif.* 1996, *10* (3), 149−159.
(48) Lemmon, E. W.; Bell, I. H.; Huber, M. L.; McLinden, M. O. NIST Standard Reference Database 23: Reference Fluid Thermodynamic and Transport Properties-REFPROP, Version 10.0, National Institute of Standards and Technology, Standard Reference Data Program. Gaithersburg 2018.

https://doi.org/10.1021/acs.iecr.2c00497
Ind. Eng. Chem. Res. 2022, 61, 9774−9784

(49) Kazakov, A.; Magee, J. W.; Chirico, R. D.; Paulechka, E.; Diky, V.; Muzny, C. D.; Kroenlein, K.; Frenkel, M. "NIST Standard Reference Database 147: NIST Ionic Liquids Database - (ILThermo)", Version 2.0; National Institute of Standards and Technology, Gaithersburg MD, 20899, 2022; https://ilthermo.boulder.nist.gov.
(50) Dong, Q.; Muzny, C. D.; Kazakov, A. F.; Diky, V.; Magee, J. W.; Widegren, J. A.; Chirico, R. D.; Marsh, K. N.; Frenkel, M. D. ILThermo: A Free-Access Web Database for Thermodynamic Properties of Ionic Liquids. *J. Chem. Eng. Data* 2007, *52* (4), 1151−1159.
(51) Iolitec. 1-n-Butyl-3-methylimidazolium hexafluorophosphate https://iolitec.de/sites/iolitec.de/files/2017-05/TDS%20IL-0011_UP%20BMIM%20PF6.pdf (accessed 2022−01−23).
(52) Iolitec. 1-n-Butyl-3-methylimidazolium tetrafluoroborate https://iolitec.de/sites/iolitec.de/files/2017-05/TDS%20IL-0012%20BMIM%20BF4.pdf (accessed 2022−01−23).
(53) Almeida, H. F. D.; Canongia Lopes, J. N.; Rebelo, L. P. N.; Coutinho, J. A. P.; Freire, M. G.; Marrucho, I. M. Densities and Viscosities of Mixtures of Two Ionic Liquids Containing a Common Cation. *J. Chem. Eng. Data* 2016, *61* (8), 2828−2843.
(54) Gao, J.; Wagner, N. J. Non-Ideal Viscosity and Excess Molar Volume of Mixtures of 1-Butyl-3-Methylimidazolium Tetrafluoroborate ([C_4mim][BF_4]) with Water. *J. Mol. Liq.* 2016, *223*, 678−686.
(55) Ahosseini, A.; Scurto, A. M. Viscosity of Imidazolium-Based Ionic Liquids at Elevated Pressures: Cation and Anion Effects. *Int. J. Thermophys.* 2008, *29* (4), 1222−1243.
(56) Shade, D.; Mounfield, W. P.; Huang, Y.; Marszalek, B.; Walton, K. S. An Automated Multi-Component Gas Adsorption System (MCGAS). *Rev. Sci. Instrum.* 2021, *92* (5), 054102.
(57) Talu, O.; Myers, A. L. Rigorous thermodynamic treatment of gas adsorption. *AIChE J.* 1988, *34* (11), 1887−1893.

https://doi.org/10.1021/acs.iecr.2c00497
Ind. Eng. Chem. Res. 2022, 61, 9774−9784